ACS APPLIED MATERIALS & INTERFACES

Research Article

www.acsami.org

# An Effective Electrical Throughput from PANI Supplement ZnS Nanorods and PDMS-Based Flexible Piezoelectric Nanogenerator for Power up Portable Electronic Devices: An Alternative of MWCNT Filler

Ayesha Sultana,[†] Md. Mehebub Alam,[†] Samiran Garain,[†] Tridib Kumar Sinha,[‡] Tapas Ranjan Middya,[†] and Dipankar Mandal*[,†]

[†]Organic Nano-Piezoelectric Device Laboratory, Department of Physics, Jadavpur University, Kolkata 700032, India

[‡]Materials Science Centre, Indian Institute of Technology (IIT), Kharagpur 721302, India

Supporting Information

**ABSTRACT:** We demonstrate the requirement of electrical poling can be avoided in flexible piezoelectric nanogenerators (FPNGs) made of low-temperature hydrothermally grown wurtzite zinc sulfide nanorods (ZnS-NRs) blended with polydimethylsiloxane (PDMS). It has been found that conductive fillers, such as polyaniline (PANI) and multiwall carbon nanotubes (MWCNTs), can subsequently improve the overall performance of FPNG. A large electrical throughput (open circuit voltage ~35 V with power density ~2.43 $\mu W/cm^3$) from PANI supplement added nanogenerator (PZP-FPNG) indicates that it is an effective means to replace the MWCNTs filler. The time constant ($\tau$) estimated from the transient response of the capacitor charging curves signifying that the FPNGs are very much capable to charge the capacitors in very short time span (e.g., 3 V is accomplished in 50 s) and thus expected to be perfectly suitable in portable, wearable and flexible electronics devices. We demonstrate that FPNG can instantly lit up several commercial Light Emitting Diodes (LEDs) (15 red, 25 green, and 55 blue, individually) and power up several portable electronic gadgets, for example, wrist watch, calculator, and LCD screen. Thus, a realization of potential use of PANI in low-temperature-synthesized ZnS-NRs comprising piezoelectric based nanogenerator fabrication is experimentally verified so as to acquire a potential impact in sustainable energy applications. Beside this, wireless piezoelectric signal detection possibility is also worked out where a concept of self-powered smart sensor is introduced.

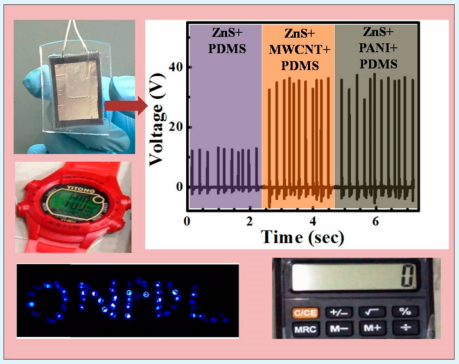


**KEYWORDS:** *wurtzite ZnS, nanorods, PDMS, polyaniline, MWCNT, flexible piezoelectric nanogenerator, energy harvester, portable electronics, wireless detection*

## INTRODUCTION

Around the last decennium, to meet the rising demand of energy and portability in everyday dependent tiny electronic gadgets, piezoelectric energy harvesting tools are gained a great attention owing to their outstanding mechano-electrical coupling effects in nanodimensional scale.[1−4] As our environment is full of ever present mechanical movements, thus several efforts have been made to harvest environmental mechanical energy sources to power up the portable devices, for example, body movement (handling, winding, pushing, stretching, bending, clapping, talking, breathing, eyelash trembling, etc.), air flow, friction, vibrations (acoustic and ultrasonic waves), and hydraulic forces (ocean waves, waterfall, or even body fluid and blood flow).[5−10] In this context, nanogenerator is expected to be best suited energy harvester that can possibly replace the bulky battery counterpart in portable electronic devices or able to directly charge up. For example, Lee et al. have demonstrated a piezoelectric nanogenerator that can scavenge energy from waving flag and also from skin wrinkling.[11] Self-charging power cells have also been made where the mechanical energy can directly converted to electrochemical energy via piezoelectric potential generation.[12,13] Cha et al. presented a sound-driven piezoelectric nanogeneator.[14] Recently, a skin sensor and a self-powered motion sensor has been reported those are capable to detect even eye ball motion and wrist bending direction.[15,16] Beside these, intensive efforts have already been paid to fabricate the piezoelectric nanogenerators, where mainly ZnO, $BaTiO_3$, and PZT are extensively examined.[17−19] Furthermore, the wurtzite structures of ZnO, GaN, ZnS, and CdSe have received vivid attraction because of their unique noncentrosymmetric structures.[20−23] Among the wurtzite classes, the noncentrosymmetric ZnS also possess a promising semiconducting property and thus suitable for wide range of applications, for instance, UV nanolasers,[24] micro force

Received: May 28, 2015
Accepted: August 18, 2015
Published: August 18, 2015




DOI: 10.1021/acsami.5b04669
ACS Appl. Mater. Interfaces 2015, 7, 19091−19097

active sensors,[22] optoelectronic devices,[25] photocatalysts,[26] ultraviolet-light sensors,[27] etc. Recently, Chen et al. have reported stress induced white and green light emissions from a ZnS based device generated from bending, stretching and even by writing.[28]Although ZnS is a nontoxic and biocompatible with superior piezoelectric property, however it is not as widely explored as ZnO, $BaTiO_3$, CdSe, GaN, and PZT in piezoelectric based energy harvesting area. Among the zinc blende and wurtzite structure of ZnS, the latter has more interesting properties, because a more sensible piezoelectricity is observed in the wurtzite structure.[29] This is due to the single independent piezoelectric coefficient in zinc blende (i.e., $e_{14}$), whereas wurtzite structure possess three independent piezoelectric coefficients (i.e., $e_{31}$, $e_{33}$, and $e_{15}$).[30] The lack of a center of symmetry in wurtzite, combined with large electromechanical coupling and nano dimensional sensitivity, results the impregnable piezoelectric properties.

In this work, we synthesize ZnS-NRs via a low temperature hydrothermal method and fabricate piezoelectric nanogenerator with ZnS-NRs and conducting supplement fillers (PANI or MWCNTs) dispersed in PDMS matrix in a simple process. The results indicate, the protonated green emeraldine salt form of PANI can be prepared via an easy process and might be alternative of MWCNTs as conducting filler to fabricate a piezoelectric nanogenerator.[31] Because the preparation of MWCNTs is quite troublesome and also difficult to disperse in the solvent systems because of weak vander Waal's forces, whereas the conductive emeraldine form of PANI can be prepared by conventional and inexpensive polymerization methodology. PDMS can help to make the device flexible for an extended range of applications. Thus, in the flexible piezoelectric nanogenerator (FPNG), ZnS-NRs are act as power generation sources and the conducting filler as dispersant, energy enhancer and conducting functional materials in PDMS matrix. The FPNG with PANI as supplement conducting filler can generate an output voltage of ~35 V and current of ~77.7 nA under the mechanical applied stress of ~13.6 kPa, where any additional treatment, such as electrical poling or annealing is avoided. Since effective electrical poling process can align the piezoelectric dipoles along an identical direction that initiates and subsequently enhances the energy harvesting performance of the device, thus it is became commonly adopted step. However, because of several disadvantages, for example, high electrical breakdown failure rate, disruption of the mechanical stability of the devices, leakage current generation, energy consumption, and more importantly safety issues, deviate from this step.[32] Furthermore, it has been found that up to 3 V is reached by capacitor charging through the PZP-FPNG that can power up several portable electronics, such as wrist watches, calculators and LCD screens. It indicates that PZP-FPNG might be alternative solution to use as a piezoelectric energy scavenger for next generation wearable and integrable electronics. The 55 blue LEDs are instantly lit up, where no external storage devices are used, so an effective means of light illumination is also being demonstrated from PZP-FPNG. Furthermore, via IR-LED trigger up from PZP-FPNG, followed by its wireless detection emphasized that the potential feasibility to as a self-powered wireless sensors.

## EXPERIMENTAL SECTION

**Materials.** Zinc acetate ($Zn(CH_3COO)_2$), thiourea ($NH_2CSNH_2$), ethylenediamine ($C_2H_4(NH_2)$) (Merck Chemicals, India), deionized water (DI) (Millipore), MWCNTs (Nanocyl S.A., Belgium), PANI (Laboratory synthesized, detail synthesis procedure and associated characterizations are provided in experimental section of Supporting Information and Figure S1), and polydimethylsiloxane (PDMS) (Sylgard 184, Dow Corning Corp., USA).

**ZnS-NRs Synthesis.** Wurtzite ZnS-NRs were synthesized via hydrothermal method at low temperature (viz., 170 °C). Initially, zinc acetate and thiourea (1:3 molar ratio) were mixed with 80 mL aqueous solution of ethylenediamine (1:1) under magnetic stirring for 20 m. Afterward, the resulting solution was poured into a Teflon lined autoclave and placed in an oven at 170 °C for 12 h. After cooling down to room temperature, the white precipitation was collected by filtration and washed several times with DI water to ensure the removal of contaminated residues. This white precipitation was then kept in oven at 80 °C for 6 h.

**FPNG Fabrication.** A detail flow diagram of FPNGs fabrication is presented in Figure 1a–d. At first, ZnS-NRs with conducting filler (PANI) in the PDMS solution were mixed by mechanical agitation in the mass ratio 2:1:100 (where PDMS and curing agent ratio = 10:1) and the mixture was poured into a Petri dish followed by placing it in vacuum condition. After the removal of air bubbles those were formed during mechanical agitation, the mixture was cured at 70 °C for 1 h to acquired the composite film (Figure 1a and b). After preparation of composite film, ~0.01 mm thick Al foils (dimension = 28 mm × 20 mm) were staked on both sides for serving as top and bottom electrodes of FPNGs (Figure 1c). Finally, the entire structure (34 mm in length, 24 mm in breadth and 2 mm in thickness) including two copper wire connection was encapsulated with thin PDMS layer (thickness ~0.2 mm) to protect from any external mechanical damage (Figure 1d) and named as PZP-FPNG.

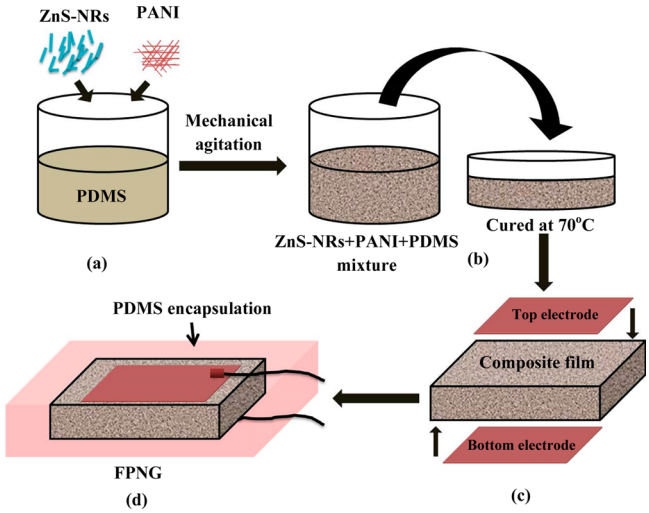


**Figure 1.** Schematic illustration of FPNG fabrication. (a) ZnS-NRs and PANI are added in PDMS solution with a mass ratio of 2:1:100. (b) The mixture containing ZnS-NRs, PANI, and PDMS are poured into a Petri dish and cured at 70 °C for 1 h to acquired the composite film. (c) The cost-effective aluminum (Al) foils are employed to served as top and bottom electrodes. (d) Finally, entire "electrode–composite–electrode" structure is encapsulated with PDMS.

In the similar way, we used MWCNTs as conducting filler instead of PANI and named as PZM-FPNG. Another reference


DOI: 10.1021/acsami.5b04669
ACS Appl. Mater. Interfaces 2015, 7, 19091–19097

sample was also prepared where conducting filler was not utilized (PZ-FPNG). It is worth mentioning that selection of amount (wt %) of ZnS-NRs and PANI or MWCNTs in PDMS was preferred as per the optimize output from FPNG (optimization of output voltage is provided in Figure S2–S4). A digital photographic image of PZP-FPNG is shown in Figure 2a, where one side Al-electrode is visible because of the

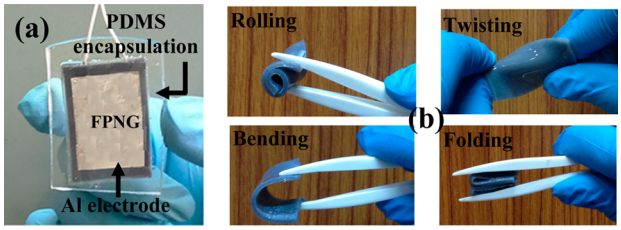


**Figure 2.** (a) A digital photographic image of PDMS encapsulated PZP-FPNG with Al electrodes. (b) The flexibility of the PZP-FPNG is demonstrated by rolling, twisting, folding and bending states.

thin and transparent PDMS coating. To demonstrate the flexibility of FPNG, rolling, twisting, folding and bending images of the composite film are provided, illustrated in Figure 2b, indicating its suitability in flexible and embedded electronics.

**Characterization.** To investigate the crystallographic structure, shape and size of the ZnS powder, X-ray diffraction (XRD, Bruker, D8 Advance), and field emission scanning electron microscope (FE-SEM) (FEI, INSPECT F 50) images were recorded. Optical properties were conducted by UV–visible (UV–vis) absorption (Shimadzu, 3110PC) and photoluminescence (PL) (Horiba, iHR320) spectra. The open circuit voltage and short circuit current from the FPNGs under repeating finger impact were recorded by a digital oscilloscope (DSO3102A, Agilent) and Nanoammeter (DNM-121, SES instruments) respectively. To demonstrate the wireless signal detection an IR-LED (TSHG8400, Vishay) and a photodiode (BPW34, Vishay) are utilized.

## RESULTS AND DISCUSSION

The XRD patterns of the as-synthesized ZnS-NRs are illustrated in Figure 3a. All diffraction peaks correspond to the planes of hexagonal wurtzite structure (JCPDS card no. 75–1534). The absence of any additional peaks indicating that contaminated crystalline specimens or additional impurities are absent in final synthesized ZnS powder.

Inset of Figure 3a presents the UV–vis absorption and PL spectra of as synthesized ZnS powder (2 mg) in ethyl alchohol

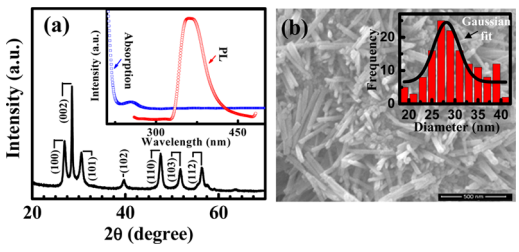


**Figure 3.** (a) XRD spectra of the as prepared ZnS-NRs and inset show the concerning UV–vis absorption and PL spectra. (b) FE-SEM image (scale bar: 500 nm) of the as synthesized ZnS-NRs and the diameter distribution is placed in the inset.

(5 mL) solution. A sharp absorption peak at 254 nm is observed that correspond to a band gap of 4.88 eV, which is greater than the bulk wurtzite ZnS (~3.88 eV) that ascribed to the quantum confinement effect.[33] In PL spectra, a strong emission at 363 nm upon excitation at 250 nm, can probably relate to the exciton emission.[34−36] The typical FE-SEM image of the as prepared ZnS powder (Figure 3b) shows a well-defined rod like structure. Inset of Figure 3b depicts the size distribution curve, the diameters are predominantly within the range of 18–42 nm where the most probable diameter of the nanorods is 28 nm.

From crystallographic wurtzite structure of ZnS (Figure 4a) it is clear that $Zn^{2+}$cations and $S^{2-}$ anions are tetrahedrally

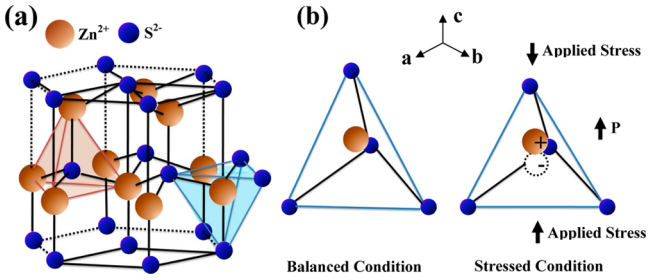


**Figure 4.** (a) Crystallographic structure of wurtzite ZnS, consists of tetrahedrally coordinated 6 $Zn^{2+}$ anions and 6 $S^{2-}$ cations per unit cell. (b) Schematics showing the piezoelectric effect in a tetrahedrally coordinated cation–anion unit. Application of stress creates displacement between positive and negative ions those possess a dipole moment (**p**) within a tetrahedron.

coordinated along the *c*-axis and the whole structure is composed by the alternative planes of these tetrahedrons. In normal state, the positive and negative charge centers of each tetrahedron coincide and hence the resultant polarization is zero. In contrast, when a stress is applied at an apex of a tetrahedron (demonstrated in Figure 4b), a relative displacement in the positive and negative charge centers possess a dipole moment. The total dipole moment (**p**) causes by all the individual unit cells in the crystal thus results in a macroscopic piezoelectric potential along *c*-axis. Thus, it is expected to fabricate a flexible piezoelectric nanogenerator (FPNG) based on the as synthesized ZnS-NRs and a polymer host, viz., polydimethylsiloxane (PDMS), as described in Figure 1a–d.

A schematic of the finger tapping process (i.e., press and release state) upon the FPNGs is demonstrated in Figure 5a. The open circuit output voltage from the PZ-, PZM- and PZP-FPNGs under repeating finger imparting (applied pressure amplitude ~13.6 kPa, estimation procedure is described in Pressure Calculation) is presented in Figure 5b. The output voltage is generated from the piezoelectric ZnS-NRs present in the FPNGs. The presence of ZnS-NRs in concerning nanocomposite specimens utilized for FPNGs fabrication are verified from XRD pattern (shown in Figure S5), where the main diffraction peak from (002) plane of wurtzite ZnS is present prominently. An enlarge view of a voltage pulse (marked with the dashed box in Figure 5b) from the PZP-FPNG is pointed in Figure 5c, the insets indicate the corresponding peak short circuit current amplitudes under the pressing (~77.7 nA) and releasing (~39.2 nA) conditions. The large positive peak is generated when the nanogenerator is subjected to compressive pressure and the negative peak occurs while returning from compressed to relaxed state. The


DOI: 10.1021/acsami.5b04669
ACS Appl. Mater. Interfaces 2015, 7, 19091–19097

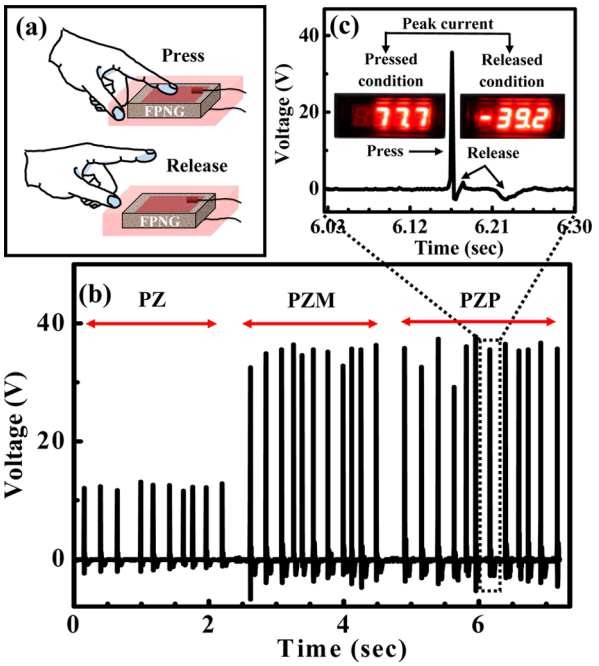


**Figure 5.** (a) Schematic of a human finger tapping process upon the FPNG. (b) Merged output voltage signals obtained by finger imparting process on PZ-, PZM-, and PZP-FPNGs. (c) An enlarge view of a voltage pulse (marked with dashed line) of PZP-FPNG. The inset shows the short circuit current values during pressure imparting and releasing process.

accumulated positive and negative charges on the top and bottom electrodes during pressed condition move in opposite direction when the pressure is released. As the FPNGs are polarized in one direction and acts as a capacitor, the stored charges on the electrodes will be dropped, resulting a negative peak. Hence the negative voltage peak is smaller than the positive peak.[37] The mechanism of the generation of piezoelectric potential within the randomly aligned ZnS-NRs can be described as follows. When a stress is applied the ZnS-NRs are subjected to compressive strain within the PDMS matrix, that creates a dipole moment within each NRs due to the noncentrocymmetric tetrahedron structures. Since the ZnS-NRs are randomly aligned, the direction of all the individual dipoles is not exactly in same as that of the stress. Rather within the nanorods, each dipole has a component in the direction of the stress. A constructive adds up of all these components results in a macroscopic potential drop along the straining direction. The open circuit voltage and short circuit current obtained from both PZP- (~35 V, ~77.7 nA) and PZM- (~35 V, ~75.4 nA) FPNGs are markedly higher than the values from PZ-FPNG (~12 V, ~4.7 nA), where conducting filler is absent. The recorded peak short circuit current values (Figure S6) under press and release condition are presented for comparison. The better output performance of PZP- and PZM, in comparison to the PZ-FPNG is mainly attributed to two facts. First, MWCNTs or PANI acting as conducting filler that results a better dispersion of ZnS-NRs[38,39] by forming a compound mixture in PDMS matrix and second it reduces the total internal resistance of the device.[38−42]

The agglomerated ZnS-NRs are formed consequently the cluster like structure as evident from the PZ composite (shown in Figure S7a). In contrast, the presence of MWCNT and PANI inhibits the agglomeration by supporting and coating the ZnS-NRs respectively, which is apparent from the better dispersion morphology in PZM and PZP composite (Figure S7b and S7c). The enhanced performance of PZP-FPNG might be the result of the rough morphology of PANI (Figure S1c) has a large specific surface area which enhances the interfacial contact area with ZnS-NRs. As the conducting emeraldine PANI exhibits a good level of conductivity (verified from the $I-V$ characteristics, Figure S1f and associated content), thus it reduces the internal resistance of the composite by forming interconnected conduction pathway within the matrix (Figure S8), yielding a high output performance. In contrast, the MWCNTs are formed themselves an electrical conducting network within the whole matrix. The comparable enhanced output from PZP- and PZM-FPNGs (hereafter, for demonstration of powering up portable electronic gadgets, PZP-FPNG is utilized) signifying that low cost and easy laboratory synthesized PANI can be alternative as conducting supplement filler instead of commercially available MWCNTs. Beside these, voltage generation from FPNGs is due to the piezoelectric potential generation from ZnS-NRs, also affirmed from the reversibility test as shown in Figure S9. Commonly, the adequate level of power generation is only feasible from piezoelectric nanogenerator reported so far after an effective electrical poling treatment as indicated in Table S1. In contrast, our device exhibits good output performance where electrical poling treatment is avoided.

The variation of output voltage and current signal from PZP-FPNG with different load resistance ($R_L$) is illustrated in Figure 6a. The output voltage amplitude increases with increasing load

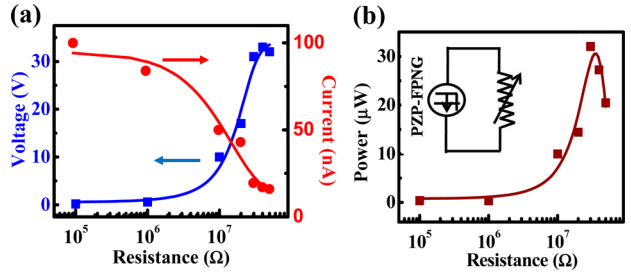


**Figure 6.** Dependence of (a) output voltage/current amplitude and (b) power output from PZP-FPNG as a function of load resistance. The inset shows an associated circuit diagram.

resistance and reached a peak value at theoretically infinite high resistance (for example, 40 MΩ, in practice) similar to open circuit voltage. Whereas, the current signal gradually decreases with increasing load resistance. The instantaneous generated power raised to a maximum value of 32 $\mu$W at load resistance of about 30 MΩ (Figure 6b). The inset of Figure 6b shows the associated circuit diagram for the measurement. The resistance dependence of voltage and current shows similar nature as previously published articles.[41,43,44]

To test the feasibility of practical implementation of the PZP-FPNG, the output piezoelectric energy created by finger impact is directly utilized to successfully operate several commercial LEDs with different color (blue, green, and red) emissions and to charge up a 1.0 $\mu$F of capacitor (a schematic circuit diagram is demonstrated in Figure 7a). To convert the ac output generated from the FPNG to a dc form, a typical bridge rectifier circuit is employed. A 1.0 $\mu$F capacitor is charged up by the three individual FPNGs, the concerning transient response is presented in Figure 7b. It implies that both charging rate and


DOI: 10.1021/acsami.5b04669
ACS Appl. Mater. Interfaces 2015, 7, 19091−19097

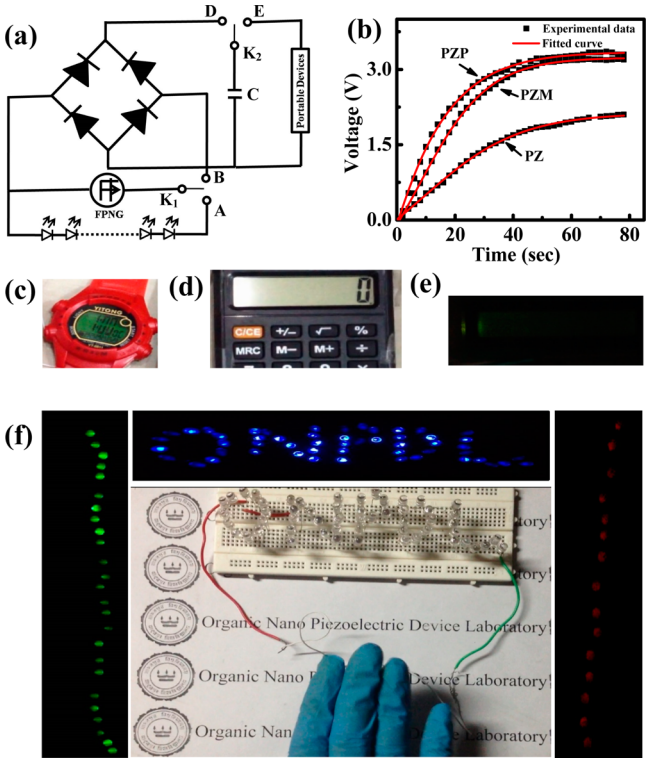


**Figure 7.** (a) A schematic circuit diagram of LED driving (when switch $K_1$ is connected to point A) and capacitor charging (switch $K_1$ connected to point B and $K_2$ connected to point D) followed by power up portable electronic devices (when switch $K_2$ is connected to point E). (b) The transient response of capacitor ($C \approx 1.0$ $\mu$F) charging from the three (PZ-, PZM-, PZP-FPNGs) by repeating human finger imparting with applied stress of ~13.6 kPa. (c–e) The photograph of portable electronic devices (c, wrist watch; d, calculator; e, LCD screen) driven by a charged 1.0 $\mu$F capacitor with PZP-FPNG. (f) Instantly driving the 55 blue LEDs (shown in the bread board) those are arranged to spell the word "ONPDL" (upper side), 25 green LEDs (left side), and 15 red LEDs (right side).

accumulation of charges are similar from PZP- and PZM-FPNG, which is significantly greater than PZ-FPNG. The charging voltages for PZ-, PZM-, and PZP-FPNGs reaches the maximum value of 2.10, 3.15, and 3.22 V within 78, 52, and 48 s, respectively. Thus, the capacitor charging result shows that the performance of both PZP- and PZM-FPNG is quite similar and much superior than the PZ-FPNG. The stored energy in the capacitor by PZP-FPNG can be used further to drive low power portable electronic devices such as wrist watch, calculator and LCD screen (Figure 7c–e, and associated Video File 1). The output power obtained from the PZM- (result not shown here) and PZP-FPNG is sufficient enough to turn on several commercial LEDs instantly, where any external power source and storage devices are not necessary. The 55 blue LEDs are arranged to spell the letters "ONPDL" those are successfully glowing (Figure 7f, Video File 2) instantly. Furthermore, PZP-FPNG can also able to lit up 15 red (Figure 7f, right side) and 25 green LEDs (Figure 7f, left side) instantly upon a simple repeating finger imparting process.

Furthermore, PZP-FPNG is tested for wireless detection of pressure impact (~13.6 kPa) in terms of output voltage/response. This application can be demonstrated by integrating a PZP-FPNG, infrared (IR) LED, photodiode and a digital oscilloscope (circuit diagram is shown in Figure 8a). The IR-

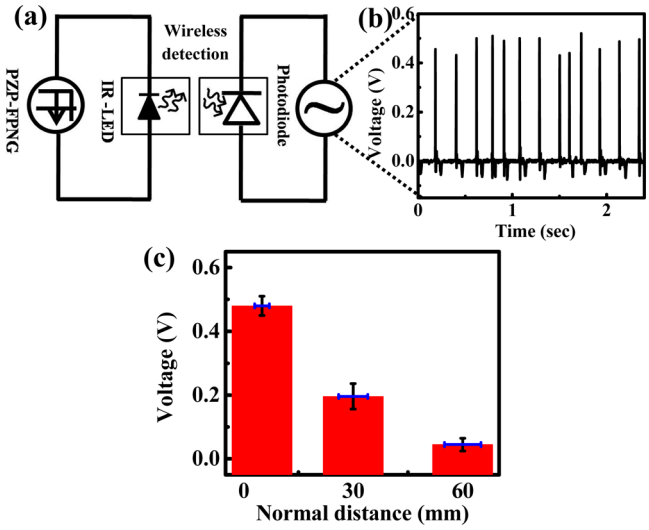


**Figure 8.** Schematic circuit diagram (a) with wireless detection of pressure impact signal (shown in panel b) via IR-LEDs and a photodiode. (c) Sensed signal of photodiode with different normal distance ($d_N$) from IR-LED.

LED was directly triggered with the power generated from PZP-FPNG to shine IR emission onto the photodiode, performed in the dark room. This IR signal acted as an external source that to be detected wirelessly via photodetector. The photodiode then responded by the IR radiation and give rise a synchronize ac signal which is recorded in oscilloscope (Figure 8b). Beside this, another measurement is carried out by changing the normal distance ($d_N$) of the IR-LED from the sensor and the IR-radiation from LED can be detected up to 60 mm of normal distance (Figure 8c).

It shows that with increasing $d_N$ from LED, the amplitude of sensed output voltage signal is gradually decreases (the original data are provided in Figure S10).This distances limitation (i.e., 60 mm) is quite sufficient enough to make an effective wireless sensor networks where PZP-FPNG might be useful to provide the associated electrical power requirement and thus energy harvesting wireless sensors network can be formed.

The performance of FPNGs are computed from the energy harvesting efficiency, $\eta$ = (output energy)/(input energy) × 100%. The overall efficiency of the PZ-, PZM-, and PZP-FPNG reached up to 0.03%, 0.096% and 0.11%, respectively (detail calculation is provide in Efficiency Calculation)

## CONCLUSION

In summary, ZnS-NRs with pure wurtzite structure are synthesized via a low temperature hydrothermal method. We fabricate piezoelectric nanogenerator with ZnS-NRs and conducting supplement fillers (laboratory synthesized PANI or commercial MWCNTs) dispersed in PDMS matrix. These fillers support for a relatively better dispersion of ZnS-NRs in PDMS matrix and leads to a heightened output response, the open-circuit voltage and short-circuit current of the PZP-FPNG reached up to ~35 V and ~77.7 nA which corresponds to a power density of ~2.43 $\mu$W/cm$^3$ under repeating finger imparting with applied stress amplitude of ~13.6 kPa. These results are also comparable to the PZM-FPNG. Beside this, both FPNGs can individually charge up a 1.0 $\mu$F capacitor up to ~3 V that enable to drive several low powered portable devices. Thus, we can conclude that PANI can be the alternative of


DOI: 10.1021/acsami.5b04669
ACS Appl. Mater. Interfaces 2015, 7, 19091–19097

MWCNTs as conducting supplement filler. More interestingly, several commercial multicolor (blue, green and red) visible and IR-LEDs are lit up instantly from PZP-FPNG, where no storage device is used. Furthermore, IR radiation emitted from LED, driven by external pressure via PZP-FPNG, is wirelessly detected at distance up to 60 mm which indicates an ability of effective transmission via fiber optics communication system. Thus, a self-powered, low cost, high-performance, flexible, piezoelectric power conversion device is fabricated in demand of growing interest in nanostructure based energy harvester. Because of excellent flexibility, robustness, and durability of FPNG, these are expected to be a potential tool for systematically harvest mechanical energy from environmental sources.

## ■ ASSOCIATED CONTENT

### Supporting Information

The Supporting Information is available free of charge on the ACS Publications website at DOI: 10.1021/acsami.5b04669.

Synthesis and characterization (FT-IR, UV−vis spectra, FE-SEM image, XRD spectra, $I-V$ characteristics curve) of PANI, optimization for the weight percentage of ZnS-NRs, PANI, and MWCNTs, pressure calculation, XRD pattern of PZ-, PZM-, and PZP-composite films, short circuit current values of PZM- and PZ-FPNGs, FE-SEM images of the PZ-, PZM-, and PZP-composites, schematic for the dispersion of ZnS-NRs and PANI in PDMS matrix, piezoelectric reversibility test of PZP-FPNG device, comparison of the FPNG performance with other reported data, voltage signals with different distance of IR LED from photodiode and efficiency calculation (PDF)

Power up the portable electronic devices (Video File 1) (AVI)

Power up LEDs (Video File 2) (AVI)

## ■ AUTHOR INFORMATION


### Corresponding Author

*Tel.: +913324146666 × 2880. Fax: +91(0)3324138917. E-mail: dipankar@phys.jdvu.ac.in.


### Author Contributions

D.M. planned the entire work and motivated to execution of the plan. A.S. wrote the manuscript. All the experiments are carried out by A.S. and M.M.A. S.G. and T.K.S. synthesized the PANI and co-operates to analyze the results. T.R.M. shared the fruitful experience that helps to finalize the manuscript. All authors finally read the manuscript and agreed for the submission.

### Notes

The authors declare no competing financial interest.

## ■ ACKNOWLEDGMENTS

This work was supported by the Science and Engineering Research Board (SERB/1759/2014- 15), Govt. of India. Ayesha Sultana is supported by State Fellowship Research Scheme (ref. No. P-1/RS/44/15). Md. Mehebub Alam (ref. No.P-1/RS/191/14) and Samiran Garain (ref. No. P-1/RS/79/13) are supported by UGC-BSR fellowship. Authors are thankful for instrumental facilities developed by DST, Govt. of India under FIST-II programme.

## ■ REFERENCES


(1) Hasan, M. R.; Baek, S.-H.; Seong, K. S.; Kim, J. H.; Park, I.-K. Hierarchical ZnO Nanorods on Si Micropillar Arrays for Performance Enhancement of Piezoelectric Nanogenerators. *ACS Appl. Mater. Interfaces* **2015**, *7*, 5768−5774.

(2) Kang, H. B.; Chang, J.; Koh, K.; Lin, L.; Cho, Y. S. High Quality Mn-Doped (Na,K)$NbO_3$ Nanofibers for Flexible Piezoelectric Nanogenerators. *ACS Appl. Mater. Interfaces* **2014**, *6*, 10576−10582.

(3) Liao, X.; Yan, X.; Lin, P.; Lu, S.; Tian, Y.; Zhang, Y. Enhanced Performance of ZnO Piezotronic Pressure Sensor through Electron-Tunneling Modulation of MgO Nanolayer. *ACS Appl. Mater. Interfaces* **2015**, *7*, 1602−1607.

(4) Mandal, D.; Henkel, K.; Schmeißer, D. Improved Performance of a Polymer Nanogenerator based on Silver Nanoparticles Doped Electrospun P(VDF−HFP) Nanofibers. *Phys. Chem. Chem. Phys.* **2014**, *16*, 10403−10407.

(5) Wang, X.; Liu, J.; Song, J.; Wang, Z. L. Integrated Nanogenerators in Biofluid. *Nano Lett.* **2007**, *7*, 2475−2479.

(6) Garain, S.; Sinha, T. K.; Adhikary, P.; Henkel, K.; Sen, S.; Ram, S.; Sinha, C.; Schmeißer, D.; Mandal, D. Self-Poled Transparent and Flexible UV Light-Emitting Cerium Complex−PVDF Composite: A High-Performance Nanogenerator. *ACS Appl. Mater. Interfaces* **2015**, *7*, 1298−1307.

(7) Zhou, J.; Gu, Y.; Fei, P.; Mai, W.; Gao, Y.; Yang, R.; Bao, G.; Wang, Z. L. Flexible Piezotronic Strain Sensor. *Nano Lett.* **2008**, *8*, 3035−3040.

(8) Meng, X. S.; Zhu, G.; Wang, Z. L. Robust Thin-Film Generator Based on Segmented Contact-Electrification for Harvesting Wind Energy. *ACS Appl. Mater. Interfaces* **2014**, *6*, 8011−8016.

(9) Xu, S.; Wei, Y.; Liu, J.; Yang, R.; Wang, Z. L. Integrated Multilayer Nanogenerator Fabricated using Paired Nanotip-to-Nanowire Brushes. *Nano Lett.* **2008**, *8*, 4027−4032.

(10) Karan, S. K.; Mandal, D.; Khatua, B. B. Self-Powered Flexible Fe-doped RGO/PVDF Nanocomposite: An Excellent Material for Piezoelectric Energy Harvester. *Nanoscale* **2015**, *7*, 10655−10666.

(11) Lee, S.; Bae, S.-H.; Lin, L.; Yang, Y.; Park, C.; Kim, S.-W.; Cha, S. N.; Kim, H.; Park, Y. J.; Wang, Z. L. Super-Flexible Nanogenerator for Energy Harvesting from Gentle Wind and as an Active Deformation Sensor. *Adv. Funct. Mater.* **2013**, *23*, 2445−2449.

(12) Xue, X.; Wang, X.; Guo, W.; Zhang, Y.; Wang, Z. L. Hybridizing Energy Conversion and Storage in a Mechanical-to-Electrochemical Process for Self-Charging Power Cell. *Nano Lett.* **2012**, *12*, 5048−5054.

(13) Xue, X.; Deng, P.; He, B.; Nie, Y.; Xing, L.; Zhang, Y.; Wang, Z. L. Flexible Self-Charging Power Cell for One-Step Energy Conversion and Storage. *Adv. Energy Mater.* **2014**, *4*, 1301329−1301334.

(14) Cha, S. N.; Seo, J.-S.; Kim, S. M.; Kim, H. J.; Park, Y. J.; Kim, S.-W.; Kim, J. M. Sound-Driven Piezoelectric Nanowire-based Nanogenerators. *Adv. Mater.* **2010**, *22*, 4726−4730.

(15) Lee, S.; Hinchet, R.; Lee, Y.; Yang, Y.; Lin, Z. − H.; Ardila, G.; Montès, L.; Mouis, M.; Wang, Z. L. Ultrathin Nanogenerators as Self-Powered/Active Skin Sensors for Tracking Eye Ball Motion. *Adv. Funct. Mater.* **2014**, *24*, 1163−1168.

(16) Chun, J.; Kang, N. − R.; Kim, J.-Y.; Noh, M.-S.; Kang, C.-Y.; Choi, D.; Kim, S. − W.; Wang, Z. L.; Baik, J. M. Highly Anisotropic Power Generation in Piezoelectric Hemispheres Composed Stretchable Composite film for Self-Powered Motion Sensor. *Nano Energy* **2015**, *11*, 1−10.

(17) Song, J.; Zhou, J.; Wang, Z. L. Piezoelectric and Semiconducting Coupled Power Generating Process of a Single ZnO Belt/Wire. A Technology for Harvesting Electricity from the Environment. *Nano Lett.* **2006**, *6*, 1656−1662.

(18) Lin, Z.-H.; Yang, Y.; Wu, J. M.; Liu, Y.; Zhang, F.; Wang, Z. L. $BaTiO_3$ Nanotubes-Based Flexible and Transparent Nanogenerators. *J. Phys. Chem. Lett.* **2012**, *3*, 3599−3604.

(19) Li, B.; You, J. H.; Kim, Y.-J. Low Frequency Acoustic Energy Harvesting using PZT Piezoelectric Plates in a Straight Tube Resonator. *Smart Mater. Struct.* **2013**, *22*, 055013−055022.




DOI: 10.1021/acsami.5b04669
*ACS Appl. Mater. Interfaces* 2015, 7, 19091−19097

(20) Wang, Z. L.; Song, J. Piezoelectric Nanogenerators Based on Zinc Oxide Nanowire Arrays. *Science* **2006**, *312*, 242−245.
(21) Lin, L.; Lai, C.-H.; Hu, Y.; Zhang, Y.; Wang, X.; Xu, C.; Snyder, R. L.; Chen, L.-J.; Wang, Z. L. High Output Nanogenerator Based on Assembly of GaN Nanowires. *Nanotechnology* **2011**, *22*, 475401−475406.
(22) Wu, J. M.; Kao, C. C. Self-Powered Pendulum and Micro-Force Active Sensors Based on a ZnS Nanogenerator. *RSC Adv.* **2014**, *4*, 13882−13887.
(23) Dong, L.; Niu, S.; Pan, C.; Yu, R.; Zhang, Y.; Wang, Z. L. Piezo-Phototronic Effect of CdSe Nanowires. *Adv. Mater.* **2012**, *24*, 5470−5475.
(24) Xiong, Q.; Chen, G.; Acord, J. D.; Liu, X.; Zengel, J. J.; Gutierrez, H. R.; Redwing, J. M.; Voon, L. C. L. Y.; Lassenand, B.; Eklund, P. C. Optical Properties of Rectangular Cross-Sectional ZnS Nanowires. *Nano Lett.* **2004**, *4*, 1663−1668.
(25) Geng, B. Y.; Liu, X. W.; Du, Q. B.; Wei, X. W. Structure and Optical Properties of Periodically Twinned ZnS Nanowires. *Appl. Phys. Lett.* **2006**, *88*, 163104−163107.
(26) Fang, Z.; Weng, S.; Ye, X.; Feng, W.; Zheng, Z.; Lu, M.; Lin, S.; Fu, X.; Liu, P. Defect Engineering and Phase Junction Architecture of Wide-Bandgap ZnS for Conflicting Visible Light Activity in Photocatalytic $H_2$ Evolution. *ACS Appl. Mater. Interfaces* **2015**, *7*, 13915−13924.
(27) Fang, X.; Bando, Y.; Liao, M.; Gautam, U. K.; Zhi, C.; Dierre, B.; Liu, B.; Zhai, T.; Sekiguchi, T.; Koide, Y.; Golberg, D. Single-Crystalline ZnS Nanobelts as Ultraviolet-Light Sensors. *Adv. Mater.* **2009**, *21*, 2034−2039.
(28) Chen, L.; Wong, M.-C.; Bai, G.; Jie, W.; Hao, J. White and Green Light Emissions of Flexible Polymer Composites under Electric Field and Multiple Strains. *Nano Energy* **2015**, *14*, 372.
(29) Moore, D.; Wang, Z. L. Growth of Anisotropic One-Dimensional ZnS Nanostructures. *J. Mater. Chem.* **2006**, *16*, 3898−3905.
(30) Catti, M.; Noel, Y.; Dovesi, R. Full Piezoelectric Tensors of Wurtzite and Zinc blende ZnO and ZnS by First-Principles Calculations. *J. Phys. Chem. Solids* **2003**, *64*, 2183−2190.
(31) Dhakras, D.; Gawli, Y.; Chhatre, S.; Wadgaonkar, P.; Ogale, S. A high Performance all-Organic Flexural Piezo-FET and Nanogenerator via Nanoscale Soft-interface Strain Modulation. *Phys. Chem. Chem. Phys.* **2014**, *16*, 22874−22881.
(32) Whiter, R. A.; Narayan, V.; Narayan, S. K. A Scalable Nanogenerator Based on Self-Poled Piezoelectric Polymer Nanowires with High Energy Conversion Efficiency. *Adv. Energy Mater.* **2014**, *4*, 1400519−1400526.
(33) Wu, Q.; Cao, H.; Zhang, S.; Zhang, X.; Rabinovich, D. Generation and Optical Properties of Monodisperse Wurtzite-Type ZnS Microspheres. *Inorg. Chem.* **2006**, *45*, 7316−7322.
(34) Yao, W.-T.; Yu, S.-H.; Pan, L.; Li, J.; Wu, Q.-S.; Zhang, L.; Jiang, J. Flexible Wurtzite-Type ZnS Nanobelts with Quantum-Size Effects: a Diethylenetriamine-Assisted Solvothermal Approach. *Small* **2005**, *1*, 320−325.
(35) Moon, H.; Nam, C.; Kim, C.; Kim, B. Synthesis and Photoluminescence of Zinc Sulfide Nanowires by Simple Thermal Chemical Vapor Deposition. *Mater. Res. Bull.* **2006**, *41*, 2013−2017.
(36) Yao, B. D.; Chan, Y. F.; Wang, N. Formation of ZnO Nanostructures by a Simple way of Thermal Evaporation. *Appl. Phys. Lett.* **2002**, *81*, 757−759.
(37) Xu, S.; Yeh, Y.-W.; Poirier, G.; McAlpine, M. C.; Register, R. A.; Yao, N. Flexible Piezoelectric PMN−PT Nanowire-Based Nanocomposite and Device. *Nano Lett.* **2013**, *13*, 2393−2398.
(38) Sun, H.; Tian, H.; Yang, Y.; Xie, D.; Zhang, Y.-C.; Liu, X.; Ma, S.; Zhao, H.-M.; Ren, T.-L. A Novel Flexible Nanogenerator Made of ZnO Nanoparticles and Multiwall Carbon Nanotube. *Nanoscale* **2013**, *5*, 6117−6123.
(39) Alam, M. M.; Ghosh, S. K.; Sultana, A.; Mandal, D. Lead-free $ZnSnO_3$/MWCNTs-Based Self-poled Flexible Hybrid Nanogenerator for Piezoelectric Power Generation. *Nanotechnology* **2015**, *26*, 165403−165409.
(40) Park, K.-I.; Lee, M.; Liu, Y.; Moon, S.; Hwang, G.-T.; Zhu, G.; Kim, J. E.; Kim, S. O.; Kim, D. K.; Wang, Z. L.; Lee, K. J. Flexible Nanocomposite Generator Made of $BaTiO_3$ Nanoparticles and Graphitic Carbons. *Adv. Mater.* **2012**, *24*, 2999−3004.
(41) Jeong, C. K.; Park, K.-I.; Ryu, J.; Hwang, G.-T.; Lee, K. J. Large-Area and Flexible Lead-Free Nanocomposite Generator Using Alkaline Niobate Particles and Metal Nanorod Filler. *Adv. Funct. Mater.* **2014**, *24*, 2620−2629.
(42) Yadav, S. K.; Jung, Y. C.; Yang, C.-M.; Ko, Y. -Il.; Yang, K.-S.; Kim, Y. A.; Cho, J. W. An Environmentally Friendly Approach to Functionalizing Carbon Nanotubes for Fabricating a Strong Biocomposite Film. *RSC Adv.* **2014**, *4*, 5382−5388.
(43) Kang, P. G.; Yun, B. K.; Sung, K. D.; Lee, T. K.; Lee, M.; Lee, N.; Oh, S. H.; Jo, W.; Seog, H. J.; Ahn, C. W.; Kim, I. W.; Jung, J. H. Piezoelectric Power Generation of Vertically Aligned lead-free $(K,Na)NbO_3$ Nanorod Arrays. *RSC Adv.* **2014**, *4*, 29799−29805.
(44) Lee, J.-H.; Yoon, H.-J.; Kim, T. Y.; Gupta, M. K.; Lee, J. H.; Seung, W.; Ryu, H.; Kim, S.-W. Micropatterned P(VDF-TrFE) Film-Based Piezoelectric Nanogenerators for Highly Sensitive Self-Powered Pressure Sensors. *Adv. Funct. Mater.* **2015**, *25*, 3203.


DOI: 10.1021/acsami.5b04669
*ACS Appl. Mater. Interfaces* 2015, 7, 19091−19097